Report

Cell Reports

Telomerase RNA *TLC1* Shuttling to the Cytoplasm Requires mRNA Export Factors and Is Important for Telomere Maintenance

Graphical Abstract

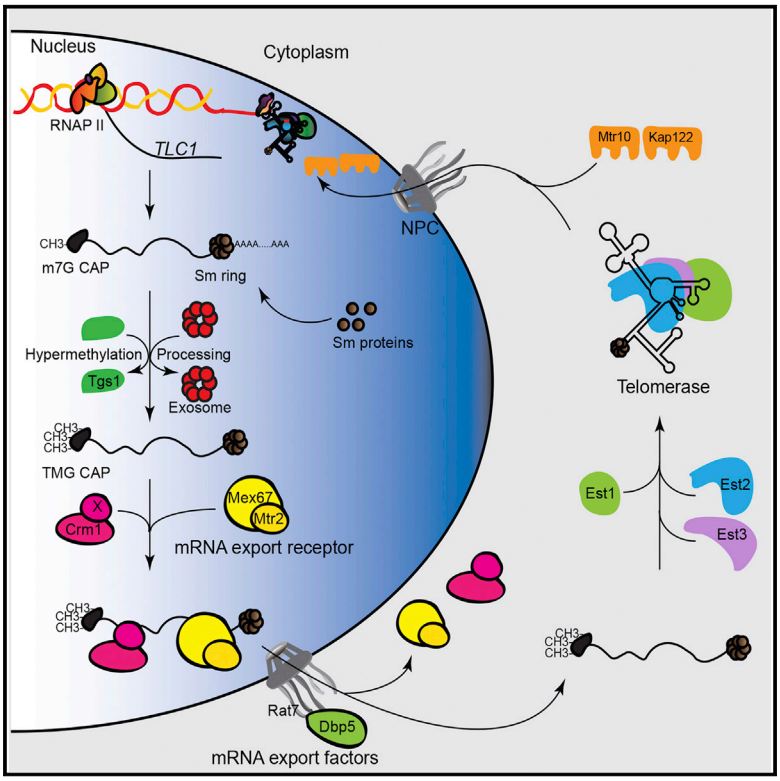

Highlights

The telomerase RNA, *TLC1*, requires mRNA export factors for nuclear exit

TLC1 physically interacts with Mex67 and Dbp5

Nuclear retention of *TLC1* leads to defects in telomerase formation

Retention of *TLC1* in the nucleus leads to telomere shortening

Authors

Haijia Wu, Daniel Becker, Heike Krebber

Correspondence

heike.krebber@biologie.uni-goettingen.de

In Brief

Telomerases protect the ends of linear chromosomes from shortening. They are composed of an RNA (*TLC1* in *S. cerevisiae*) and several proteins. During telomerase maturation, *TLC1* shuttles to the cytoplasm and recruit proteins. The mature complex is subsequently reimported into the nucleus to fulfill its function on telomeres. Wu et al. now uncover the export machinery for *TLC1* and reveal the importance of this step by finding short telomere defects in export factor mutants.

Wu et al., 2014, Cell Reports 8, 1630–1638
September 25, 2014 ©2014 The Authors
http://dx.doi.org/10.1016/j.celrep.2014.08.021

OPEN ACCESS
CellPress

Cell Reports
Report

Telomerase RNA *TLC1* Shuttling to the Cytoplasm Requires mRNA Export Factors and Is Important for Telomere Maintenance

Haijia Wu,[1] Daniel Becker,[1] and Heike Krebber[1,*]
[1]Abteilung für Molekulare Genetik, Institut für Mikrobiologie und Genetik, Göttinger Zentrum für Molekulare Biowissenschaften (GZMB), Georg-August Universität Göttingen, 37077 Göttingen, Germany
*Correspondence: heike.krebber@biologie.uni-goettingen.de
http://dx.doi.org/10.1016/j.celrep.2014.08.021

SUMMARY

Telomerases protect the ends of linear chromosomes from shortening. They are composed of an RNA (*TLC1* in *S. cerevisiae*) and several proteins. *TLC1* undergoes several maturation steps before it is exported into the cytoplasm to recruit the Est proteins for complete assembly. The mature telomerase is subsequently reimported into the nucleus, where it fulfills its function on telomeres. Here, we show that *TLC1* export into the cytoplasm requires not only the Ran GTPase-dependent karyopherin Crm1/Xpo1 but also the mRNA export machinery. mRNA export factor mutants accumulate mature and export-competent *TLC1* RNAs in their nuclei. Moreover, *TLC1* physically interacts with the mRNA transport factors Mex67 and Dbp5/Rat8. Most importantly, we show that the nuclear export of *TLC1* is an essential step for the formation of the functional RNA containing enzyme, because blocking *TLC1* export in the *mex67-5 xpo1-1* double mutant prevents its cytoplasmic maturation and leads to telomere shortening.

INTRODUCTION

Telomerases are enzymatic ribonucleoprotein complexes that antagonize the constant loss of the eukaryotic chromosome ends upon replication by the synthesis of repetitive DNA sequences. The telomerase of *Saccharomyces cerevisiae* is composed of an RNA molecule (*TLC1*), which provides a scaffold for the assembly of the protein components (Gallardo et al., 2008). The main catalytic enzyme is the reverse transcriptase Est2 (Lingner et al., 1997). In addition, regulatory subunits such as Est1 and Est3 are also required for the telomerase activity (Evans and Lundblad, 1999). All Est proteins are essential components of the telomerase as also reflected in their names: "*e*ver shorter *t*elomeres." The mature nuclear telomerase at telomeres requires the Yku70/80 complex. In its absence, the telomerase shuttles in and out of the nucleus and is localized to the cytoplasm at steady state (Gallardo et al., 2008). The association of the Est proteins has been suggested to occur in the cytoplasm (Gallardo et al., 2008). The cytoplasmic assembly step of the telomerase, which might prevent immature complexes from occupying telomere ends, requires the nucleocytoplasmic shuttling of *TLC1* that was reported to utilize the Ran GTPase-dependent exportin Xpo1/Crm1 and the importins Mtr10 and Kap122 (Gallardo et al., 2008).

As a transcript of RNA polymerase II, *TLC1* becomes polyadenylated like an mRNA; however, the tail is removed during maturation (Chapon et al., 1997). At steady state, 5%–10% of all *TLC1* transcripts contain an ~80-nt-long poly(A) tail, which is accomplished by the same machinery that polyadenylates mRNAs (Chapon et al., 1997). Moreover, maturation of the *TLC1* RNA requires the entrance into the nucleolus, where hypermethylation of the cap structure by Tgs1 takes place (Gallardo et al., 2008; Seto et al., 1999). Furthermore, the Sm binding site is required for the nuclear exosome-mediated processing of *TLC1* from different polyadenylated precursors into its mature form (Coy et al., 2013). The mature *TLC1* is subsequently exported into the cytoplasm for full maturation.

Other transcripts of RNA polymerase II (e.g., mRNAs) recruit processing and mRNA export factors cotranscriptionally, among them the mRNA export receptor heterodimer Mex67-Mtr2, which mediates the nuclear export through the nuclear pore complex (NPC) (Niño et al., 2013; Strambio-De-Castillia et al., 2010). On the cytoplasmic side of the NPC, directionality of transport is generated by the displacement of Mex67-Mtr2 from the mRNA by the DEAD box RNA helicase Dbp5 and its cofactors Gle1, IP_6, and Rat7/Nup159 (Tieg and Krebber, 2013).

Although the nuclear export of *TLC1* was reported to depend on the Ran GTPase-dependent Xpo1/Crm1 (Gallardo et al., 2008), no telomere shortening defects have been reported for mutants of Crm1/Xpo1, indicating that this export receptor might not be the only responsible transporter for the nuclear export of *TLC1* RNAs. As a polymerase II transcript, it seems possible that *TLC1* might also receive components of the mRNA export machinery during transcription. Therefore, we addressed this question and found that indeed the nuclear export of *TLC1* in addition to Xpo1/Crm1 requires the mRNA export machinery. Strikingly, upon mutation of both export pathways, we find that the severely inhibited export of *TLC1* subsequently leads to telomerase formation defects and consequently to telomere shortening.

RESULTS AND DISCUSSION

The Nuclear Export of *TLC1* Is Inhibited in mRNA Export Mutants

The mature *TLC1* RNA is composed of 1,157 nt. This large size, which is similar to the size of a typical mRNA in yeast, and its negative charge is a challenge for the passage through the hydrophobic NPC (Strambio-De-Castillia et al., 2010). Therefore, export receptors are required that coat the transport cargo to allow export. The nuclear export of *TLC1* was shown to depend on Crm1/Xpo1 (Gallardo and Chartrand, 2008). Surprisingly, no telomere shortening defects have been reported for mutants of Crm1/Xpo1, which suggests that the nuclear export of *TLC1* RNAs is not required for the assembly of functional telomerases or that other currently unknown export factors exist. As a polymerase II transcript, it seems possible that *TLC1* might interact with the mRNA export machinery. To investigate a requirement of mRNA export factors in the transport of *TLC1* to the cytoplasm, we compared the cellular localization of the *TLC1* RNA and bulk mRNAs by fluorescent in situ hybridization (FISH) experiments in wild-type, *xpo1-1*, and different mRNA export-defective mutants. In wild-type cells, *TLC1* is localized within the nucleus in several discrete foci as reported earlier (Gallardo et al., 2008) (Figure S1A). In contrast, *xpo1-1* cells shifted to the restrictive temperature showed a nuclear signal (Figure S1A). Strikingly, a similar accumulation was also detected in the mRNA export factor mutants *mex67-5*, *rat7-1*, and *rat8-2* (Figure S1A), suggesting defects in the nuclear export of *TLC1*. To better visualize this phenotype, we repeated this assay in the *yku70* deletion strain in which the telomerase is cytoplasmic at steady state (Gallardo et al., 2008). In this background, ~40% of *TLC1* accumulates in the nuclei of all three mRNA export mutants, as compared to ~20% in *yku70*Δ, clearly revealing nuclear export defects (Figures 1A and 1B). A nuclear, but not nucleolar, accumulation of *TLC1* was detected (Figures S1B and S1C), suggesting that *TLC1* is not affected in its nucleolar maturation steps.

xpo1-1 mutants show also slight mRNA export defects (Stade et al., 1997), raising the possibility that Xpo1 might not directly be involved in the *TLC1* export. It has been reported earlier that overexpression of the mRNA export factor *DBP5* rescues the mRNA export defects of *xpo1-1* (Hodge et al., 1999). To investigate if this would also rescue the *TLC1* mislocalization, we overexpressed *DBP5* in *xpo1-1* and found that while the mRNA export defect was abrogated, *TLC1* was still mislocalized to the nucleus, indicating that the nuclear export signal (NES) export function of Xpo1 has a direct impact on the *TLC1* nuclear export (Figure S1D).

To detect the *TLC1* export defects in a distinct approach, we isolated total RNA of yeast cytoplasmic fractions and amplified *TLC1*. While the *TLC1* RNA was clearly detectable in wild-type cells and in the unrelated translation termination factor mutant *sup45-2*, it was significantly reduced in *mex67-5*, *rat7-1*, and *rat8-2* cells (Figure 1C). Together, these results suggest that *TLC1* RNAs require the mRNA export machinery for their transport into the cytoplasm.

mRNA Export Factors Physically Interact with *TLC1*

An involvement of the mRNA export factors in *TLC1* transport was further supported by the findings that *TLC1* physically interacts with Mex67 and Dbp5/Rat8 in RNA coimmunoprecipitation (IP) analyses. Crm1/Xpo1, Est1, and Est2 served as a positive control and eIF4G as a negative control (Figure 1D). This shows that not only Crm1/Xpo1 but also the mRNA export factors physically bind to *TLC1*. Moreover, it suggests that the interaction period of *TLC1* with mRNA export factors is rather similar to that of Crm1/Xpo1 and possibly restricted to the export phase. In contrast to that, Est1 and Est2, although precipitated to a lesser extent, show a strong (1,000-fold enriched) interaction with *TLC1* (Figure 1D), which one could speculate might be due to the fact that these proteins bind for a longer time period, as they are factors present on the matured telomerase, and that the export factors bind several transport cargoes while the Est-proteins bind only *TLC1*. It is currently unclear if Mex67 for its interaction with *TLC1* requires adaptor proteins such as Npl3 or Nab2, like in mRNA export (Niño et al., 2013; Strambio-De-Castillia et al., 2010). However, it is equally possible that the interaction is rather direct, like in ribosomal subunit transport, where Mex67 contacts the 5S rRNA directly (Yao et al., 2007). Taken together, the mislocalization of *TLC1* in mRNA export mutants and its physical interaction with the mRNA export factors suggest their involvement in the nuclear export of *TLC1*.

TLC1 Export Mutants Accumulate Fully Processed RNAs

To exclude that defects in processing might be responsible for the nuclear export defects, we investigated the amount of the processed and export competent *TLC1* RNA in export mutants. We observed that the ratio of the *TLC1* to the U6 RNA, a transcript of RNA polymerase III, was comparable to wild-type in all export mutants, suggesting that the mRNA export mutants are not defective in the transcription of *TLC1* (Figure 2A).

Analogous to mRNAs, *TLC1* RNAs are polyadenylated upon transcription termination. The poly(A) tail is, however, subsequently removed, so that in an average only 5%–10% of all *TLC1* molecules contain a poly(A) tail (Chapon et al., 1997). To monitor potential defects in the maturation of *TLC1*, which would be reflected by an increase of the immature form of the *TLC1* RNA, we determined the ratio of the total RNA and the unprocessed RNA by quantitative RT-PCRs (qRT-PCRs) with specific primers (Figure 2B) and found that significantly less immature *TLC1* was detectable in all export mutants (Figure 2C), which is also visible in northern blot analyses (Figure S2), suggesting that only fully processed and export competent *TLC1* RNAs accumulate in the nucleus, waiting to be exported. These data suggest that the processing of the immature form of *TLC1* occurs prior to its export and that only the processed form is exported to the cytoplasm and accumulates in the export mutants. Also, since the amount is not reduced, it seems that the mature form is stable and not prone to degradation, possibly because in the export mutants, it is packaged for export and in this form not accessible to RNases.

Both the NES and the mRNA Export Pathways Act on One *TLC1* RNA

To investigate whether *TLC1* can either be exported by the NES export pathway or the mRNA export pathway or if both pathways contribute to the export of one *TLC1* RNA, we performed IPs in wild-type cells and cells mutated either in *XPO1* or in *MEX67*

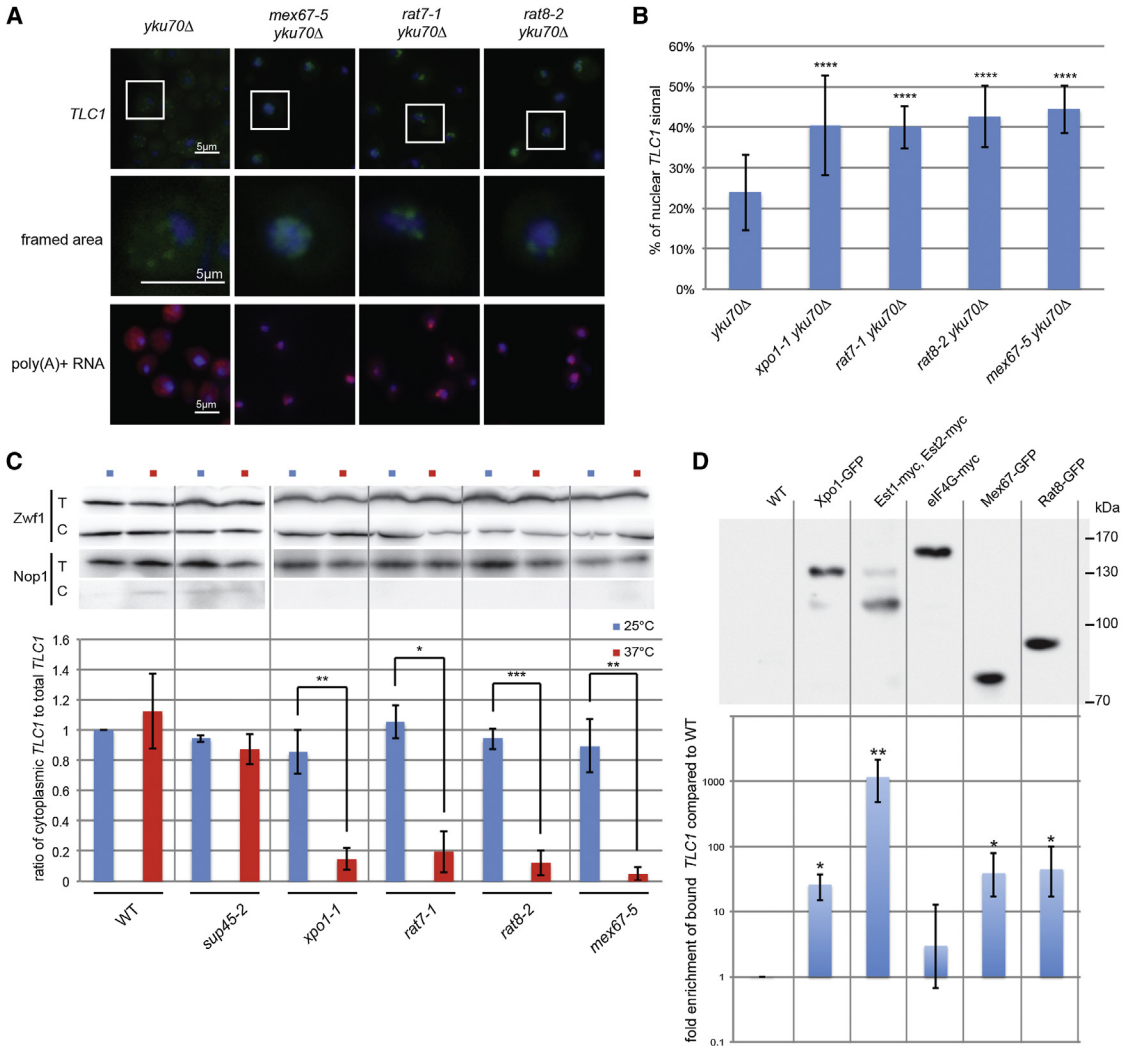

Figure 1. Nuclear Export of *TLC1* Requires mRNA Export Factors

(A) FISH experiments in the *yku70Δ* background reveal *TLC1* (in green) nuclear export defects. The indicated strains were grown to the logarithmic growth phase before they were shifted to 37°C for 1 hr. FISH experiments with a digoxigenin (DIG)-labeled *TLC1* probe were performed and detected with fluorescein isothiocyanate-labeled DIG antibodies. The DNA was stained with Hoechst 33342. Single cells are shown enlarged in the framed area. Bulk mRNA was detected with a Cy3-labeled oligo $d(T)_{50}$ probe.

(B) Quantification of the signal intensity of 20 cells is shown. p values were calculated according to an unpaired two-tailed t test.

(C) Reduced amounts of *TLC1* are detected in the cytoplasm of mRNA export factor mutants. Nucleocytoplasmic fractionation experiments were carried out with the indicated strains. Cells were grown to the log phase. Then they were either retained at 25°C or shifted to 37°C for 1 hr. The top shows a western blot from the total lysate (T) and the cytoplasmic fraction (C) probed with anti-Zwf1 to stain a cytoplasmic protein and anti-Nop1 to stain a nuclear protein. The bottom shows the results from three different qRT-PCR experiments in which *TLC1* was amplified from the RNA extracted from the cytoplasmic fraction compared to the total RNA. The error bars show the SD.

(D) Physical interactions of *TLC1* and mRNA export factors. Western blot analyses of the immunoprecipitated proteins from strains expressing the indicated tagged proteins are shown that were pulled with anti-myc and anti-GFP (top). The western blot was probed with a mixture of anti-myc and anti-GFP. The bottom shows RNA IP experiments that reveal a physical interaction of Xpo1, Est1, Est2, Mex67, and Rat8 with *TLC1* via qRT-PCR. The translation factor eIF4G served as a negative control. The binding of *TLC1* to the proteins compared to the total RNA and the untagged wild-type control is shown. One representative western blot is shown. Three qRT-PCR experiments are shown in the bottom.

The error bars shown in this figure show the SD of at least three experiments. p values shown in (C) and (D) were calculated according to a paired two-tailed t test compared to eIF4G.

and compared the amount of *TLC1* associated with Xpo1 or Mex67. Interestingly, defects in either of these pathways, which both lead to the nuclear accumulation of *TLC1* (Figure 1), increased the *TLC1* association of both export factors (Figure 2D). This result shows that both export factors are connected via *TLC1* and either export factor defect affects the other, which supports a model in which both export factors act on different positions of *TLC1* to cooperatively export this large RNA.

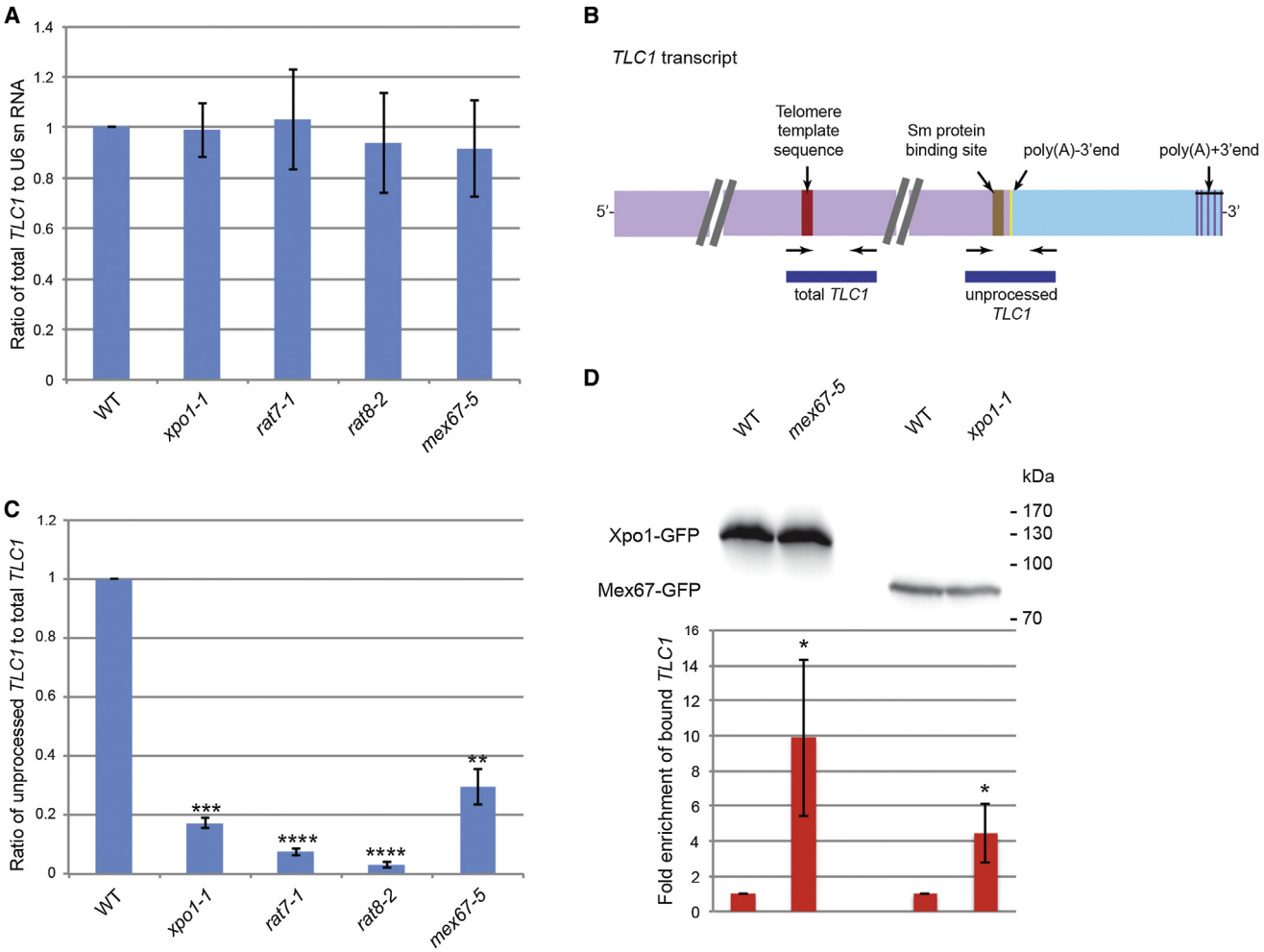

Figure 2. Mutations in mRNA Export Factors Result in an Increased Amount of Processed *TLC1*

(A) All *TLC1* export-defective mutants are not impaired in the total level of *TLC1* RNA. The indicated strains were grown to log phase before shifted to 37°C for 1 hr. The total RNA was isolated from the cells, and qRT-PCR experiments revealed the ratio of the total *TLC1* in comparison to the amount of the U6 small nuclear RNA.

(B) Primers used to detect the total *TLC1* (mature and immature) and the unprocessed *TLC1*. A schematic representation of the *TLC1* RNA is shown that includes the mature *TLC1* (pink area) and the immature *TLC1* (pink and blue area). The primer pairs (in black) that amplify either all *TLC1* molecules present in the cell (total *TLC1*) or the immature forms (unprocessed *TLC1*) are indicated.

(C) Fully processed *TLC1* RNAs accumulate in the *TLC1* export mutants. The indicated strains were grown to log phase before they were shifted to 37°C for 1 hr. The total RNA was isolated from the cells and qRT-PCR experiments revealed the decreased ratio of the unprocessed *TLC1* in comparison to the total *TLC1* in the *TLC1* export mutants.

(D) IP analyses reveal connected export activities of Xpo1 and Mex67. Western blots of immunoprecipitates of Xpo1-GFP or Mex67-GFP in wild-type (WT) or *mex67-5* or *xpo1-1* are show (top). qRT-PCR experiments were performed to determine the amount of coprecipitated *TLC1* RNA (bottom). All experiments were done at least three times, and the error bars show the SD.

The error bars depicted in this figure show the SD. p values were calculated according to a paired two-tailed t test.

Defects in mRNA Export Factors Prevent Proper Telomerase Formation

Upon entry of *TLC1* in the cytoplasm, maturation of the telomerase continues and proteins including Est1 and Est2 associate. However, because its export is affected in *xpo1-1* and the mRNA export mutants, *TLC1* is depleted from the cytoplasm, and one would expect that lesser amounts of Est1 and Est2 should be tethered to the telomerase in the nucleus. Indeed, we found that the wild typical nuclear localization of Est1 and Est2 is significantly decreased in all export mutants (Figure 3A) to similar amounts of ~30% (Figure 3B). In other words, 70% of Est1 and Est2 are localized to the cytoplasm as compared to ~40% in the wild-type, indicating defects in the cytoplasmic assembly of the telomerase. Interestingly, none of the export mutants showed a comparably low percentage of nuclear signals as detected in *tlc1Δ*, which might be an indication that both export pathways, the Ran-dependent Crm1/Xpo1 and the mRNA export pathway, contribute to the transport of *TLC1* to the cytoplasm.

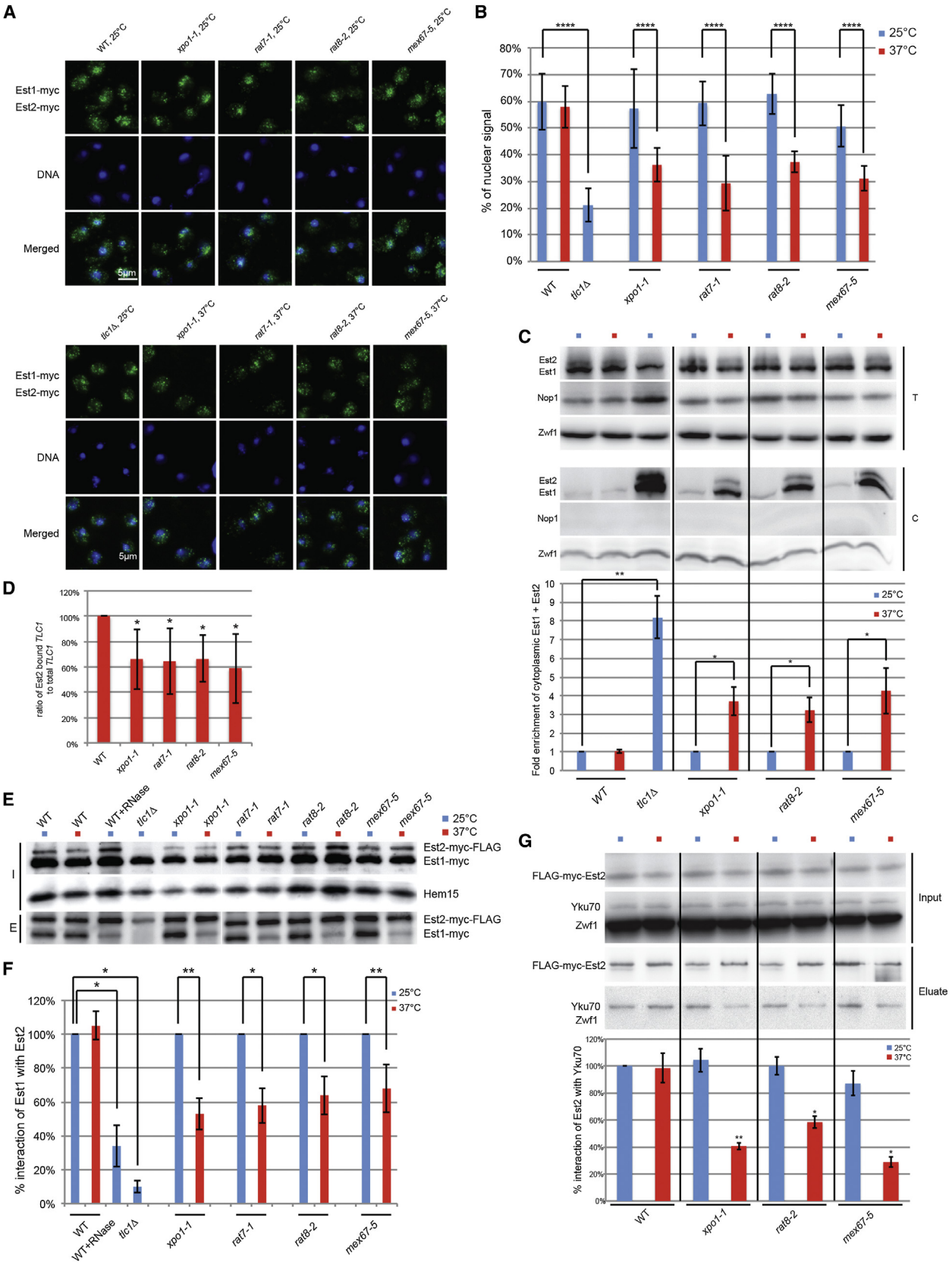

(legend on next page)

A similar result was also obtained in nucleocytoplasmic fractionation experiments in which the cytoplasmic level of Est1 and Est2 clearly increased (~4-fold) in all *TLC1* export mutants (Figure 3C).

To analyze these potential defects in telomerase assembly in the *TLC1* export mutants directly, we determined the amount of *TLC1* that is bound to Est2 by RNA IP experiments and found a ~40% reduction of *TLC1* RNA bound to Est2 in all export mutants relative to wild-type, indicating a requirement for *TLC1* translocation to the cytoplasm for its binding to Est2 (Figure 3D). These assembly defects are further confirmed by interaction studies of Est1 with Est2. Both proteins interact with each other in the cytoplasm upon binding to *TLC1* (Gallardo and Chartrand, 2008). We coimmunoprecipitated Est1 bound to Est2 in wild-type cells and compared the precipitates from wild-type to the export factor mutants (Figure 3E). Quantification of these interactions revealed a ~40% reduced interaction of Est1 and Est2 in all export mutants (Figure 3F), reflecting the cytoplasmic depletion of *TLC1*. Even stronger results were obtained when cells were either treated with RNase A, which destroys the *TLC1* scaffold, or when the IP analyses were done in cells lacking *TLC1* (*tlc1Δ*) (Figures 3E and 3F). Notably, when related to the loading control Hem15, it became apparent that the cellular amounts of Est1 and Est2 are relatively stable in all analyzed mutants (Figure S3). However, some degradation seems to occur in *tlc1Δ* and might suggest that Est1 and Est2 are possibly more susceptible to degradation when not incorporated into the telomerase complex.

These findings suggest that less telomerase is reimported into the nucleus to bind to the telomere ends for telomere maintenance. To finally show that directly, we investigated the incorporation of Est2 into the mature telomere at the telomere ends by IP of Est2 with the telomere protein Yku70 (Gallardo et al., 2008). In contrast to wild-type cells, in which both proteins show a clear interaction, this interaction is reduced to ~40%–60% in *xpo1-1*, *rat8-2*, and *mex67-5* mutants (Figure 3G). These results clearly show that less functional telomerase is generated in the *TLC1* export mutants. Taken together, these experiments reinforce the requirement of the mRNA export machinery for the nuclear export of *TLC1* and support the requirement for the cytoplasmic translocation of *TLC1* for further maturation steps.

Blocking the Export of *TLC1* Results in Shorter Telomere Ends

Our data suggest that *TLC1* RNAs are transported in a combined action of two cellular transport pathways, the Ran GTPase-dependent Crm1/Xpo1 pathway and the mRNA export pathway. The inhibition of one of the export pathways still allows enough export of this RNA into the cytoplasm to support the formation of sufficient intact telomerases to prevent telomere shortening. Inhibiting both *TLC1* export pathways should prevent sufficient export and result in a dysfunctional telomerase leading to severe telomere shortening. Indeed, *xpo1-1 mex67-5 yku70Δ* cells show a significant further increase of the nuclear *TLC1* RNA signal as compared to the single mutants in the presence of *yku70Δ* and to *yku70Δ* (Figure 4A), suggesting that both pathways cooperate to transport *TLC1*. This strong nuclear export block of *TLC1* in the double mutant is also reflected by a further increase of the fully processed *TLC1* RNA compared to the amount detected in the single mutants (Figure 4B). This effect is not due to a decrease of the amount of *TLC1* (Figure S4A). Furthermore, the amount of mislocalized Est1 and Est2 is increased in *xpo1-1 mex67-5* double mutant (~60% cytoplasmic) as compared to the single mutants (~40% cytoplasmic) (Figure 4C). These additive effects of defects in *XPO1* and *MEX67* on the export of *TLC1* further support a model in which both pathways join forces to collectively transfer *TLC1* to the cytoplasm.

Consequently, subsequent Southern blot analyses in which telomere shortening can be visualized revealed severe defects in telomere maintenance, reflected in the shortening of the telomere, for the double mutant *xpo1-1 mex67-5*, but not the single mutants (Figure 4D). Wild-type and *yKu70* deletion strains served as negative and positive controls, respectively, for the progressive shortening of the telomeres. All strains were grown at the semipermissive temperature of 32°C for *xpo1-1 mex67-5* for 30 and 60 generations. This effect is not due to a decrease of the amount of *TLC1* and reduced level of the Est proteins at this temperature (Figures S4B and S4C).

Figure 3. Mutations in mRNA Export Factors Result in Telomerase Formation Defects

(A) Est1 and Est2 are mislocalized to the cytoplasm in *TLC1* export mutants. Immunofluorescence experiments were performed with the indicated strains either retained at 25°C or shifted to 37°C for 1 hr. Hoechst 33342 stains the DNA and indicates the nucleus.

(B) Comparison of cells in the permissive and the restrictive situation (25°C versus 37°C and WT versus *tlc1Δ*) reveal a highly significant increase of mislocalized telomerase components Est1 and Est2. Quantification of the nuclear signal compared to the total signal of at lest 50 cells per strain and condition from Figure 3A are shown. p values were calculated according to an unpaired two-tailed t test.

(C) Nucleocytoplasmic fractionation experiments reveal increased cytoplasmic level of Est1 and Est2. Nucleocytoplasmic fractionation experiments were carried out with the indicated strains. Cells were grown to the log phase. Then, they were either retained at 25°C or shifted to 37°C for 1 hr. The top shows a western blot from the total lysate (T) and the cytoplasmic fraction (C) probed with anti-Zwf1 to stain a cytoplasmic protein and anti-Nop1 to stain a nuclear protein. The bottom shows the results from three different qRT-PCR experiments in which *TLC1* was amplified from the RNA extracted from the cytoplasmic fraction compared to the total RNA.

(D) The interaction of the *TLC1* RNA and Est2 is reduced in *TLC1* export mutants. RNA IP experiments were performed with Est2 in the indicated strains grown at 25°C to the log phase and then shifted to 37°C for 1 hr. The Est2-bound *TLC1* RNA was then determined by qRT-PCR and compared to the total *TLC1* and to 25°C.

(E) The interaction of Est1 and Est2 is disturbed in *TLC1* export mutants. Anti-FLAG IP experiments with FLAG-myc-tagged Est2 and myc-tagged Est1 are shown in western blot analyses with anti-myc.

(F) Quantification of three independent experiments, one of which is shown in (E).

(G) Less mature telomerase is assembled in the *TLC1* export mutants. Western blots of a representative FLAG-IP analysis of Yku70 with FLAG-myc-tagged Est2 is shown from the indicated strains that were grown to log phase and then shifted to 37°C for 1 hr (top). Zwf1 served as a negative control.

All error bars depicted in this figure show the SD of at least three different experiments. p values were calculated according to a paired two-tailed t test.

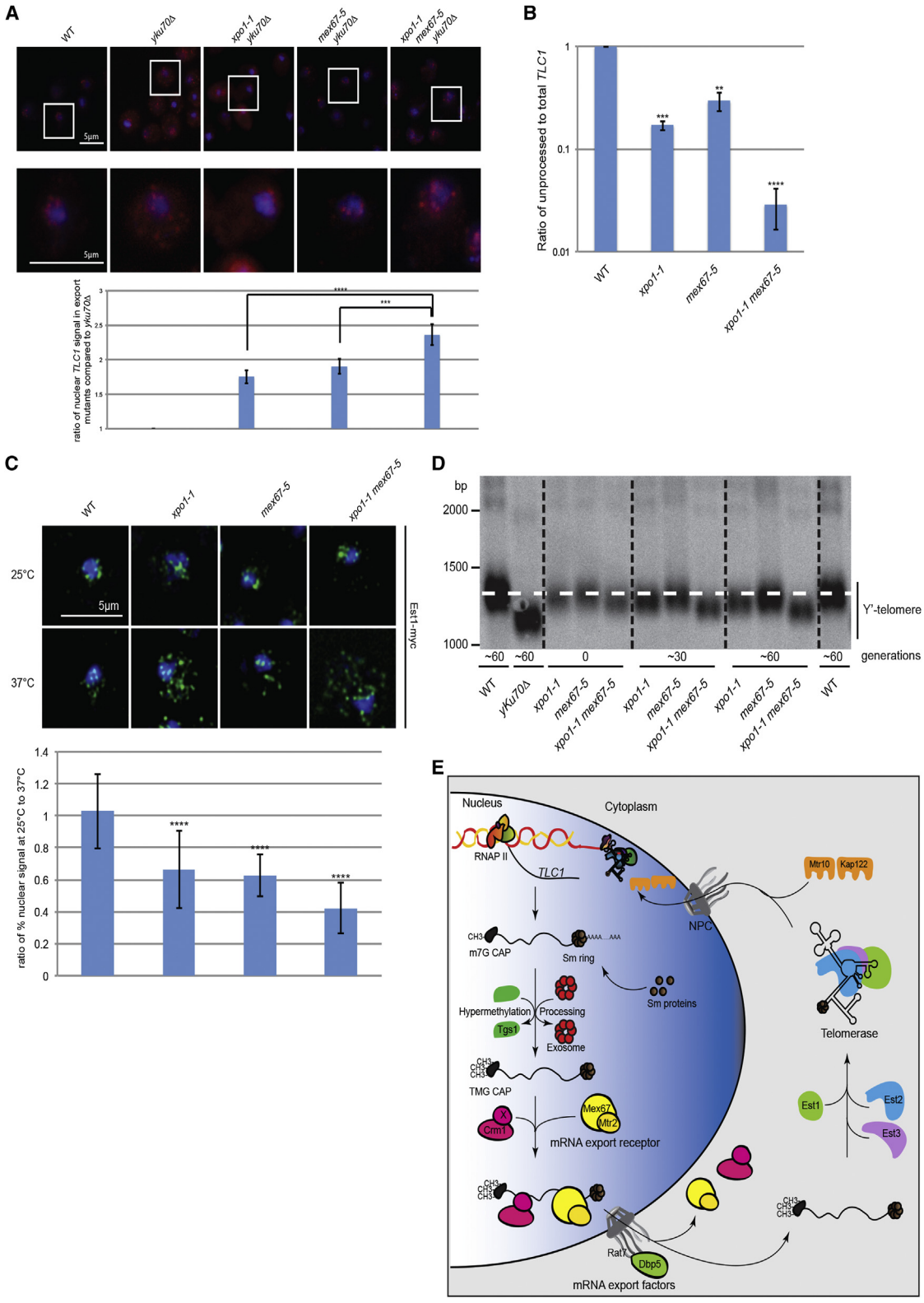

Figure 4. Mutations in mRNA Export Factors Lead to the Shortening of Telomeres

(A) FISH experiments reveal an export block of *TLC1* RNA in the double mutant *xpo1-1 mex67-5*. The experiment was performed in the *yKu70*Δ background. All indicated strains were grown to the logarithmic growth phase at 25°C before the cells were shifted to 37°C for 1 hr. *TLC1* was detected with Cy3-labeled

(legend continued on next page)

Interestingly, while *mex67-5* after 60 generations shows no effect on telomere shortening, a very slight effect was visible for *xpo1-1* (Figure 4D). This might be due to the fact that this mutant has also slight mRNA export defects, which might be caused by the mislocalized mRNA export factor Dbp5 (Hodge et al., 1999). Strikingly, although these mRNA export defects are rescued by the overexpression of *DBP5*, the *TLC1* export defects remain (Figure S1D). Also, the telomere shortening defects remain in the presence of high-copy *DBP5* (Figure S4D), which clearly shows that both the NES and the mRNA export pathways participate in the *TLC1* export.

In sum, these data reveal the dependence of *TLC1* to exit the nucleus for the maturation of the telomerase, which requires that several export factors join forces to produce a functional telomerase (Figure 4E). It has been suggested earlier that the cytoplasmic assembly step of the telomerase might have evolved to prevent that immature complexes occupy the telomere ends (Gallardo et al., 2008). However, if the shuttling is indeed essential for telomere maintenance was not clear, because Crm1/Xpo1 mutants did not affect telomere length. Our findings that telomere ends cannot be maintained in the double mutant *mex67-5 xpo1-1*, in which the nuclear export of *TLC1* is prevented (Figure 4), clearly show a necessity for the cytoplasmic shuttling of *TLC1* and indicate that the nuclear maturation is not sufficient to create functional telomerases that support telomere maintenance.

Thus, our results support a model in which upon completion of the nuclear maturation the *TLC1* RNA is exported into the cytoplasm (Figure 4E). Its export is mediated by the Ran GTPase-dependent karyopherin Crm1/Xpo1 and the mRNA export factors Mex67, Dbp5/Rat8, and Nup159/Rat7. Both pathways contribute to the nuclear export of *TLC1* and when mutated prevent its export, which ultimately leads to telomerase formation defects and subsequently to telomere shortening.

EXPERIMENTAL PROCEDURES

Oligonucleotides, Strains, and Plasmids

Oligonucleotides, yeast strains, and plasmids used in this study are listed in the Supplemental Experimental Procedures. Detailed descriptions on how strains were constructed as well as detailed growth conditions can be found in the Supplemental Experimental Procedures.

FISH and Immunofluorescence

The experiments were essentially performed as described earlier (Hackmann et al., 2014). For further details, see the Supplemental Experimental Procedures.

IP Analyses, RNA Co-IP, and qRT-PCR

The experiments were essentially performed as published earlier (Hackmann et al., 2014). Homogenized cell lysates were incubated with the indicated antibodies and immobilized on matrix beads. The protein interaction partners were detected by western blot analyses. The RNA interaction partners were further quantified by using qRT-PCR. For further details, see the Supplemental Experimental Procedures.

Signal Detection and Quantification

Detailed description of western blot and Southern blot assays, fluorescent signals, and qRT-PCR analyses can be found in the Supplemental Experimental Procedures. p values are indicated as follows: ****$p < 0.0001$, ***$0.0001 < p < 0.001$, **$0.001 < p < 0.01$, *$0.01 < p < 0.05$.

Detection of Telomere Shortening

Southern blot analyses were performed to detect the length of the telomeres. For additional details, see the Supplemental Experimental Procedures.

SUPPLEMENTAL INFORMATION

Supplemental Information includes Supplemental Experimental Procedures and four figures and can be found with this article online at http://dx.doi.org/10.1016/j.celrep.2014.08.021.

AUTHOR CONTRIBUTIONS

H.W. and H.K. designed the study. H.W. and D.B. performed the experiments. H.W., D.B., and H.K. analyzed the data. H.K. wrote the manuscript.

ACKNOWLEDGMENTS

We are grateful to P. Chartrand, R. Lill, V. Lundblad, P.A. Silver, and K. Weis for providing strains or antibodies. We thank H. Bastians and the members of the H.K. lab for discussions. This work was supported by grants from the Deutsche Forschungsgemeinschaft (DFG) awarded to H.K. and the SFB 860.

oligonucleotide probes and the DNA was stained with Hoechst 33342. Quantification of the nuclear signals of 20 cells/mutant in comparison to *yku70Δ* is shown (bottom).

(B) Increased accumulation of the processed *TLC1* RNAs in the *xpo1-1 mex67-5* double mutant. The indicated strains were grown to log phase before they were shifted to 37°C for 1 hr. The total RNA was isolated from the cells and qRT-PCR experiments revealed the decreased ratio of the unprocessed *TLC1* in comparison to the total *TLC1* in the *TLC1* export mutants. p values were calculated according to a paired two-tailed t test.

(C) The double mutant *xpo1-1 mex67-5* shows an increased cytoplasmic accumulation of Est1. Colocalization experiments of Est1-myc (green) and the DNA (blue) in the logarithmic growing indicated strains either retained at 25°C or shifted to 37°C for 1 hr are shown (top). Quantification of the nuclear signals of 20 cells/condition is shown and set into relation (bottom). p values shown in (A) and (C) were calculated according to an unpaired two-tailed t test. All error bars depicted in this figure show the SD of at least three different experiments.

(D) Southern blot analyses reveal the progressive shortening of telomeres in mRNA export factor mutants. The indicated single and double mutant strains were grown for the indicated generations at the semipermissive temperature of 32°C. The DNA was extracted, digested, and separated on an agarose gel. The length of the Y′ telomere was determined by Southern blot analyses with a DIG-labeled probe.

(E) Model for the life cycle of *TLC1*. *TLC1* is generated in the nucleus by RNA polymerase II (RNAP II). Upon association of the Sm ring, the RNA is processed and the poly(A) tail removed by the nuclear exosome. The CAP is hypermethylated and a trimethylguanine (TMG) CAP is generated. The Ran-dependent nuclear export signal (NES) export receptor Crm1/Xpo1 associates via a currently unknown NES containing protein (X). Proper nuclear export additionally requires the mRNA export machinery; the export receptor heterodimer Mex67-Mtr2 associates and supports transport through the nuclear pore complex (NPC). Upon transit Mex67-Mtr2 is displaced by the DEAD box RNA helicase Dbp5 that is located at the cytoplasmic filaments of the NPC, where it interacts with Rat7/Nup159. The subsequent cytoplasmic maturation of the telomerase requires the association of several proteins including Est1, Est2, and Est3. The mature telomerase is reimported into the nucleus via the importins Mtr10 and Kap122, where it finally associates with the telomere ends.

Received: April 11, 2014
Revised: July 9, 2014
Accepted: August 8, 2014
Published: September 11, 2014

REFERENCES

Chapon, C., Cech, T.R., and Zaug, A.J. (1997). Polyadenylation of telomerase RNA in budding yeast. RNA *3*, 1337–1351.

Coy, S., Volanakis, A., Shah, S., and Vasiljeva, L. (2013). The Sm complex is required for the processing of non-coding RNAs by the exosome. PLoS ONE *8*, e65606.

Evans, S.K., and Lundblad, V. (1999). Est1 and Cdc13 as comediators of telomerase access. Science *286*, 117–120.

Gallardo, F., and Chartrand, P. (2008). Telomerase biogenesis: The long road before getting to the end. RNA Biol. *5*, 212–215.

Gallardo, F., Olivier, C., Dandjinou, A.T., Wellinger, R.J., and Chartrand, P. (2008). TLC1 RNA nucleo-cytoplasmic trafficking links telomerase biogenesis to its recruitment to telomeres. EMBO J. *27*, 748–757.

Hackmann, A., Wu, H., Schneider, U.M., Meyer, K., Jung, K., and Krebber, H. (2014). Quality control of spliced mRNAs requires the shuttling SR proteins Gbp2 and Hrb1. Nat Commun *5*, 3123.

Hodge, C.A., Colot, H.V., Stafford, P., and Cole, C.N. (1999). Rat8p/Dbp5p is a shuttling transport factor that interacts with Rat7p/Nup159p and Gle1p and suppresses the mRNA export defect of xpo1-1 cells. EMBO J. *18*, 5778–5788.

Lingner, J., Hughes, T.R., Shevchenko, A., Mann, M., Lundblad, V., and Cech, T.R. (1997). Reverse transcriptase motifs in the catalytic subunit of telomerase. Science *276*, 561–567.

Niño, C.A., Hérissant, L., Babour, A., and Dargemont, C. (2013). mRNA nuclear export in yeast. Chem. Rev. *113*, 8523–8545.

Seto, A.G., Zaug, A.J., Sobel, S.G., Wolin, S.L., and Cech, T.R. (1999). Saccharomyces cerevisiae telomerase is an Sm small nuclear ribonucleoprotein particle. Nature *401*, 177–180.

Stade, K., Ford, C.S., Guthrie, C., and Weis, K. (1997). Exportin 1 (Crm1p) is an essential nuclear export factor. Cell *90*, 1041–1050.

Strambio-De-Castillia, C., Niepel, M., and Rout, M.P. (2010). The nuclear pore complex: bridging nuclear transport and gene regulation. Nat. Rev. Mol. Cell Biol. *11*, 490–501.

Tieg, B., and Krebber, H. (2013). Dbp5 - from nuclear export to translation. Biochim. Biophys. Acta *1829*, 791–798.

Yao, W., Roser, D., Köhler, A., Bradatsch, B., Bassler, J., and Hurt, E. (2007). Nuclear export of ribosomal 60S subunits by the general mRNA export receptor Mex67-Mtr2. Mol. Cell *26*, 51–62.